https://doi.org/10.30799/jnst.365.26110101 J. Nanosci. Tech. - Volume 11 Issue 1 (2026) 1022–1026

Share Your Innovations through JACS Directory

Journal of Nanoscience and Technology

Visit Journal at https://www.jacsdirectory.com/jnst

ISSN: 2455-0191

Rietveld Structure Refinement and Effect of Sintering Temperature on Elastic Properties of Cobalt Nano Ferrite

Ravindra N. Chikhale[1,*], Vikas S. Shinde[2]

[1]Department of Physics, J.S.M. College, Alibag, Raigad– 402 201, Maharastra, India.
[2]Department of Physics, K.E.S. Anandibai Pradhan Science College, Nagothane, Raigad – 402 107, Maharastra, India.

ARTICLEDETAILS

Article history:
Received 17 December 2025
Accepted 12 January 2026
Available online 18 January 2026

Keywords:
Nano Ferrite
Sintering Temperature
Sol-Gel
Auto Combustion
Elastic Moduli

ABSTRACT

Cobalt ferrite nanoparticles were synthesized by citrate sol-gel auto combustion technique and sintered at 400 °C, 700 °C, and 900 °C. The structural characterization of the samples was done by using XRD, SEM and FTIR. The XRD and FTIR analysis clearly showed the formation of a cubic spinel structure for all samples sintered at different temperatures. The crystallite size increased from 15.99 nm to 69.08 nm while the grain size increased from 56.28 nm to 107.54 nm with increase in sintering temperature. It was observed that lattice parameters increase with an increase in sintering temperature. From the FTIR spectra, the higher frequency band in the range of 500-600 cm^{-1} confirmed the vibrations due to M-O stretching at the tetrahedral site, while the lower band in the range 400-500 cm^{-1} confirmed the vibrations due to M-O stretching at the octahedral site. In the present work force constants (K_t, K_0), elastic velocities (V_l, V_t, V_m), elastic moduli (Y, G, B), Poisson's ratio, and Debye temperature were evaluated.

1. Introduction

Spinel ferrite materials are metal oxides with spinel structures that have the general chemical formula M (Fe_2O_4), where M is a divalent cation metal ion such as Ni^{2+}, Mn^{2+}, Mg^{2+}, Zn^{2+}, Co^{2+}, Cu^{2+} [1]. Unit cell of spinel ferrites consists of 32 O^{2-} ions, 16 Fe^{3+} ions and 8 divalent metal irons i.e. total 56 ions which is 8 times greater than the total ions contained in the general formula. Hence the unit cell of spinel ferrite contains 8 formula units [2,3].

In the crystal structure of spinel ferrite, divalent and trivalent metal cations can occupy either tetrahedral A site or octahedral B site. Depending on this site occupancy these ferrites can be classified as normal, inverse, and mixed ferrite. In normal spinel ferrites, all the divalent metal cations occupy A sites and all trivalent metal cations occupy B sites. In the inverse spinel ferrites, half of the trivalent cations occupy A sites while the remaining half and divalent cations occupy B sites. In mixed spinel ferrite, the divalent and trivalent metal cations are randomly distributed among A and B sites [4,5].

In recent years, spinel ferrites have attracted the attention of many researchers due to specific properties such as high electrical resistance, high chemical/thermal stability, high permeability, and mechanical properties. Due to these properties, spinel ferrites play some roles such as in biomedical fields, chemical sensors, data storage devices, magnetic actuators, magnetic ceramics, magnetic hyperthermia, manufacture contaminant nano-adsorbents, magnetic resonance imaging (MRI), power transformers, sensing applications, solar cells, storage devices, and supercapacitors [6]. Cobalt ferrite is a member of the inverse spinel ferrite and has various advantages due to its strong cubic magneto crystalline anisotropy, high coercivity, moderate saturation magnetization, high electrical resistivity, high Curie temperature, excellent chemical stability and low cost. These properties make them an ideal candidate for use in permanent magnets, energy and information storage devices, microwave absorption, chemical industry like biosensors and gas sensors and biomedical applications [7,8].

Co ferrite nanoparticles were synthesized by various methods such as sol–gel auto combustion, hydrothermal, solvothermal, co-precipitation, Solid-State Synthesis, thermal decomposition and microwave combustion methods etc., [9,10]. Among all these methods, sol–gel auto-combustion is found as the simplest method having the advantages of low cost, low sintering temperature, rapid synthesis, low-external energy consumption, good purity, porous structure, good chemical homogeneity, large surface area, good stoichiometric control, controllable particle size, etc., [11,12].

The chemical, physical and magnetic properties of spinel ferrites largely depend on crystalline structure, cation distribution at tetrahedral and octahedral sites, composition and microstructure and therefore can be tuned through suitable substitutions, synthesis route and sintering temperature variations [13].

More et al. synthesized $Ni_{0.25}Cu_{0.55}Zn_{0.20}Fe_2O_4$ nano ferrite by using a sono-chemical method, was sintered at different (200 °C, 400 °C, 600 °C, and 800 °C). It has been observed that the cubic phase of $Ni_{0.25}Cu_{0.55}Zn_{0.20}Fe_2O_4$ is generated and is unaffected by temperature changes. FTIR reveals that with the increase in the sintering temperature there is shift in the tetrahedral and octahedral band position. FESEM and TEM images revealed the nanocrystals exhibit irregular shapes which transformed into cubic and hexagonal morphology with the increase in the sintering temperature [14].

Xavier et al., synthesized $CoFe_2O_4$ nanoparticles by using a sol-gel technique that was sintered at different temperatures (300 °C, 400 °C, 500 °C and 700 °C). It has been observed that the cubic phase of $Ni_{0.25}Cu_{0.55}Zn_{0.20}Fe_2O_4$ is generated and is unaffected by temperature changes. A negligible presence of hematite (α -Fe_2O_3) phase is detected in all the samples. The crystallite size of the samples increases with the increase in the sintering temperature. The TEM image shows that the nanoparticles are spherical in shape and slightly agglomerated. The FTIR analysis corroborates the spinel characteristics of the samples [15].

Han et al., synthesized $Zn_{0.5}Co_{0.5}Fe_2O_4$ ferrite powder by sol–gel method at different sintering temperatures (600 °C, 700 °C, 800 °C, 900 °C and 1000 °C). It has been observed that the change of sintering temperature does not change the crystal structure of ferrite. As the temperature increases, the lattice constant does not change much, but the crystallite size and experimental density increase, the porosity decreases, From the SEM image analysis it is seen that the particle size of the sample is significantly larger than the crystallite size. The FTIR analysis confirm the spinel characteristics of the samples [16]

Literature review shows that Temperature is one of the key parameters in the synthesis of a system of magnetic nanoparticles and can considerably affect the arrangement of atoms in the crystal structure. Consequently, the magnetic, elastic, and structural properties are strongly impacted. Keeping this in mind, cobalt ferrite nanoparticles with formula

*Corresponding Author:chikhaleravi@gmail.com(Ravindra N. Chikhale)

https://doi.org/10.30799/jnst.365.26110101

Cite this Article as: Ravindra N. Chikhale, Vikas S. Shinde, Rietveld structure refinement and effect of sintering temperature on elastic properties of cobalt nano ferrite, J. Nanosci. Tech. 11(1) (2026) 1022-1026.

$CoFe_2O_4$ has been prepared by sol–gel auto combustion method and studied the effect of the different sintering temperatures such as 400 °C, 700 °C, and 900 °C on structural and elastic properties of $CoFe_2O_4$ nanoparticles. The prepared samples were characterized by X-ray diffractometer (XRD), High-resolution field emission scanning electron microscopy (HR-SEM) and Fourier transforms infrared spectroscopy (FTIR).

2. Experimental Methods

Cobalt ferrite ($CoFe_2O_4$) nanoparticles were synthesized by citrate sol-gel auto combustion technique [17]. In this work, $Fe(NO_3)_3.9H_2O$ (Merck, ≥ 99.95%), $Co(NO_3)_2.6H_2O$ (Merck, ≥ 99.95%), and citric acid monohydrate $C_6H_5O_7$ (Merck, ≥ 99.95%) were used as raw materials without any further purification. Different steps involved in the sol–gel auto-combustion synthesis of $CoFe_2O_4$ spinel ferrite nanoparticles are given in Fig. 1.

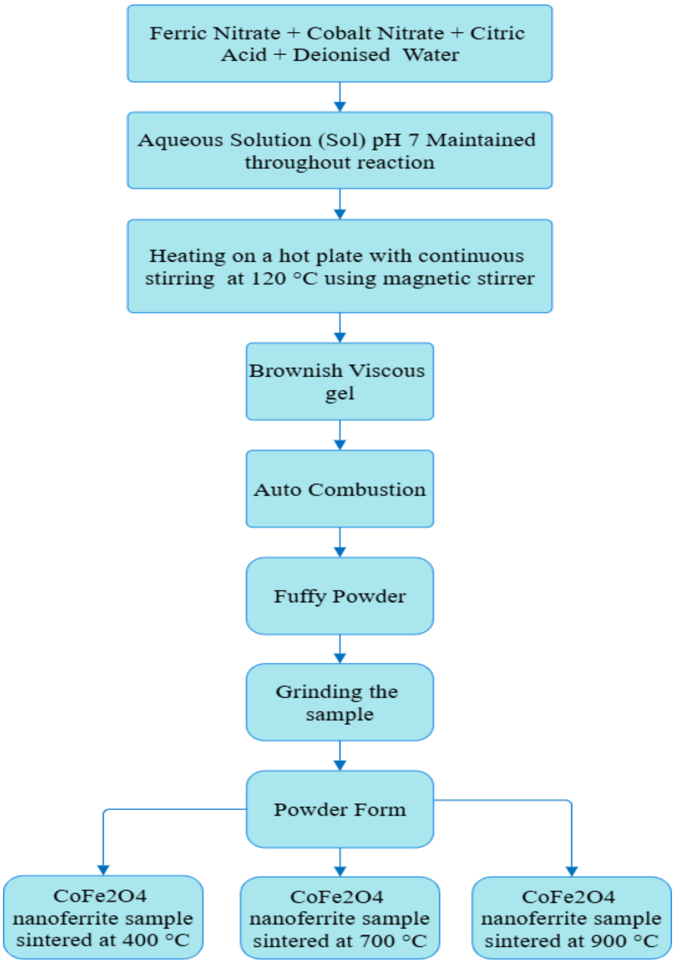

Fig. 1 Steps involved in the sol-gel auto-combustion synthesis of $CoFe_2O_4$ nano ferrite

3. Results and Discussion

3.1 XRD Analysis

X-ray diffraction (XRD) for prepared $CoFe_2O_4$ nano ferrite samples sintered at different temperatures (400 °C, 700 °C, and 900 °C) was recorded between 20° and 80°. It has been observed reflecting peaks indexed as (220), (311), (212), (400), (331), (422), (511/333) (440), (531), (442), (620), (533), (622) and (444) according to standard JCPDS card #22-1086 [18,19]. Rietveld refined XRD data of $CoFe_2O_4$ nanoparticles sintered at 400 °C, 700 °C, and 900 °C performed using Full-Proof software as shown in Fig. 2(a-c).

The XRD pattern of the synthesized nanoparticles shows sharp and intense diffraction peaks with narrow full width at half maxima (FWHM) is evidence of the crystalline nature. XRD pattern of prepared sample at different sintering temperature not showing any notable impurity peak, indicating the formation of the pure cubic spinel ferrite structure [20]. The intensity of the XRD peak was increased (FWHM was decreased) as sintering temperature increased from 400 °C to 900 °C, hence the crystallite size found to be increased. The overall $\chi 2$ values from Rietveld refinement are 1.54, 1.14 and 1.36 for the $CoFe_2O_4$ samples sintered at 400 °C, 700 °C, and 900 °C respectively, which is indicative of good agreement between the reference data and the experimental data.

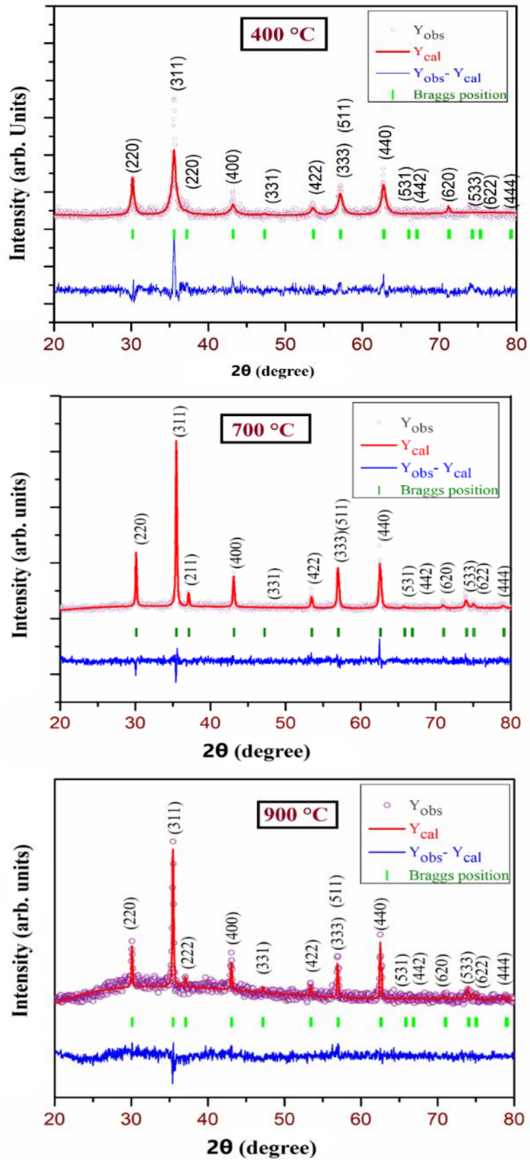

Fig. 2 Rietveld refinement of XRD data of CoFe2O4 nano ferrite sintered at (a) 400 °C; (b) 700 °C and (c) 900 °C

Structural parameters obtained from Rietveld refinement of $CoFe_2O_4$ nano ferrite sintered at 400 °C, 700 °C, and 900 °C are given in Table 1.

The crystallite size (D), Lattice volume (V), and X-ray density (ρ_x) were estimated using following relations [19, 21].

$$D = \frac{0.9\,\lambda}{\beta\cos\theta} \quad (1)$$

$$V = a^3 \quad (2)$$

$$\rho_x = \frac{8M}{N_A V} = \frac{8M}{N_A a^3} \quad (3)$$

where θ = Bragg's angle of maximum intensity peak, λ = Wavelength of Cu-Kα radiation, β = angular line width at high maximum intensity (FWHM), M = Molecular weight of the composition, and N_A = Avogadro's number.

Table 1 Structural parameters obtained from Rietveld refinement of $CoFe_2O_4$ nano ferrite sintered at 400 °C, 700 °C and 900 °C

Parameters	Sintering Temperature		
	400 °C	700 °C	900 °C
X^2	1.54	1.14	1.36
a = b = c (Å)	8.3752	8.3930	8.3975
V (Å^3)	587.4706	591.2440	592.1907
FWHM (β) (degree)	0.4940	0.1433	0.1144
(D) (nm)	15.99	55.14	69.08
ρ_m (g/cm^3)	5.3055	5.2717	5.2632
(D_m) (nm)	56.28	65.79	107.54

https://doi.org/10.30799/jnst.365.26110101

While calculating crystallite size, the highest intensity peak (311) was considered for prepared samples sintered at different temperatures. The calculated values of crystallite size, lattice volume, X-ray density, and grain size for $CoFe_2O_4$ nano ferrite for various sintering temperatures have been noted in Table 1. The Rietveld analysis shows that the lattice parameters and lattice volume increases with increasing sintering temperature. The crystallite size increases as the sintering temperature increases because the diffusion between grains occurs easily at higher temperatures. Atomic activity and mobility are temperature dependent and found to increase with increase in sintering temperature. The lattice defects and strain decrease with increase in sintering temperatures. Hence, atoms are easily agglomerated for higher sintering temperature and grain size increases [15,16,22]. As the sintering temperature increases from 400 °C to 900 °C the X-ray density decreases because of an increase in lattice constant (lattice volume). The lattice constant depends on many factors like crystal size, grain growth, and lattice strain and for spinel ferrites generally increases as sintering temperature increases [23,24].

3.2 HR-SEM Analysis

High-resolution scanning electron microscope (HR-SEM) (Resolution 1.2 nm and magnification 12x – 10^5x) was used to study surface morphology and microstructural analysis of the $CoFe_2O_4$ nano ferrite sintered at different temperatures. The SEM micrographs and the histogram of grain size distribution of $CoFe_2O_4$ nanoparticles sintered at 400 °C, 700 °C, and 900 °C are shown in Fig. 3. ImageJ software was used to measure the size of particles.

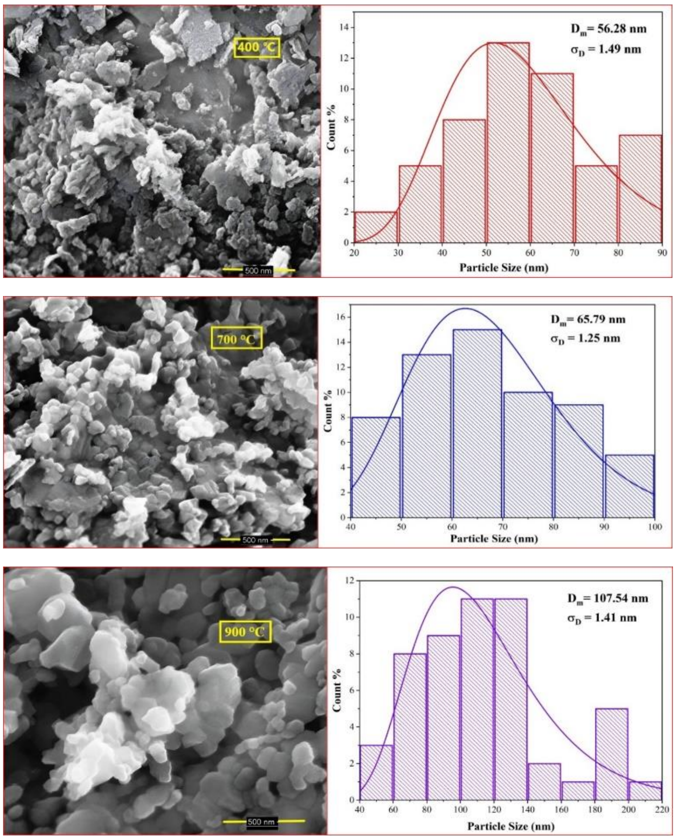

Fig. 3 SEM images and histograms of $CoFe_2O_4$ nano ferrite sintered at (a) 400 °C; (b) 700 °C and (c) 900 °C

The SEM images show that particles are homogeneously distributed with non-uniform size. The size of the grains was measured by using ImageJ software. The particle size distribution for prepared samples was estimated by fitting the size histogram with a log-normal function represented by the following equation [25].

$$f(D) = \frac{1}{\sqrt{2\pi}\sigma D} exp\left[\frac{ln^2\left(\frac{D}{D_0}\right)}{2\sigma^2}\right] \quad (4)$$

where, D_0 = median diameter and σ = size dispersity,

The mean diameter D_m and standard deviation σ_D estimated from the following equations [25],

$$D_m = \exp\left[\ln(D_0) + \frac{\sigma^2}{2}\right] \quad (5)$$

$$\sigma_D = \mathrm{Dm}[\exp(\sigma^2) - 1]^{1/2} \quad (6)$$

The average grain size was observed to be 56.28 nm, 65.79 nm and 107.54 nm along with standard deviation (σ_D) 1.49 nm, 1.25 nm, and 1.41 nm for $CoFe_2O_4$ nanoparticles sintered at 400 °C, 700 °C, and 900 °C respectively. It is observed that for prepared samples sintered at different temperatures the average grain size is larger than the average crystallite size determined from XRD data. Because every particle is formed due to agglomeration of several crystallites [26].

3.3 FTIR Study

The Fourier Transform Infrared (FTIR) spectra $CoFe_2O_4$ nano ferrite sintered at 400 °C, 700 °C, and 900 °C were recorded in the range of 400 - 1000 cm^{-1} and are shown in Fig. 4.

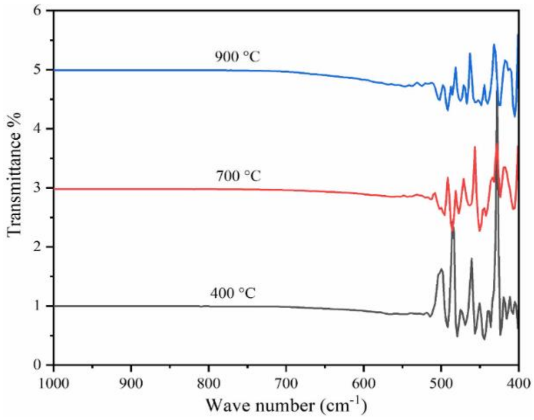

Fig. 4 FTIR spectra $CoFe_2O_4$ nano ferrite sintered at 400 °C, 700 °C, and 900 °C

FTIR spectra show vibration band in the range 600–550 cm^{-1} corresponds to the stretching vibrational mode of M-O in the tetrahedral sites (A) and lowest band in the range 450–400 cm^{-1} corresponds to the stretching vibrational mode of M-O in the octahedral sites (B) [27, 28]. Presence of vibrational bands corresponding to A and B sites confirm formation of spinel ferrite structure [29].

Force constants K_t and K_0 at A and B sites were calculated using following relation [30].

$$K_t = 4\pi^2c^2\vartheta_1^2\mu \quad (7)$$

$$K_0 = 4\pi^2c^2\vartheta_0^2\mu \quad (8)$$

where, μ = Reduced mass of Fe^{3+} and O^{2-} ions ($\mu = 2.065 \times 10^{-26}$ Kg/mol), c = Velocity of electromagnetic wave ($c = 2.99 \times 10^8$ m/s)

Average force constant (K) estimated as,

$$K = (K_t + K_0)/2 \quad (9)$$

Absorption frequencies ϑ_t and ϑ_0 corresponding to tetrahedral (A) and octahedral (B) sites were measured from FTIR spectra and listed in Table 2. This present study observed that shifting of ϑ_t and ϑ_0 towards lower frequency with increase in sintering temperature. The frequency shifts are mainly attributed due to variation of cations distribution with respect to sintering temperature, gain size, and method of synthesis [31]. Eqs (7) and (8) show that force constant (K_t and K_0) is proportional to vibrational frequency (ϑ_t and ϑ_0) are found to decreases with increasing sintering temperature. This decrease may result from the movement of cations between A and B sites and change in bond lengths [32].

Table 2 Tetrahedral stretching frequency (ϑ_t) and octahedral stretching frequency (ϑ_0), force constant K_t and K_0 at A and B sites, and average force constant (K) of $CoFe_2O_4$ spinel ferrites sintered at 400 °C, 700 °C and 900 °C

Parameters	Sintering Temperature		
	400 °C	700 °C	900 °C
ϑ_t (cm^{-1})	564.29	553.57	546.88
ϑ_0 (cm^{-1})	407.3	406.53	405.21
K_t (N/m)	231.84	223.11	217.75
K_0 (N/m)	120.78	120.33	119.55
K (N/m)	176.31	171.72	168.65

3.4 Elastic Properties

Elastic properties of cobalt ferrite sintered at different sintering temperatures were studied using FTIR and XRD data. The stiffness constant (C_{11}) was calculated using the following relation [33].

$$C_{11} = \frac{K}{a} \quad (10)$$

where, a = Lattice constant

https://doi.org/10.30799/jnst.365.26110101

The velocity of longitudinal wave (V_L), velocity of shear wave (V_S), mean velocity (V_m), longitudinal modulus (Y), rigidity Modulus (G), Poisson's ratio (σ), stiffness constant (C_{12}), Bulk modulus (B), and Debye temperature (θ_D) estimated from following equations [33].

$$V_L = \left(\frac{C_{11}}{\rho}\right)^{1/2} \quad (11)$$

$$V_S = \frac{V_L}{\sqrt{3}} \quad (12)$$

$$V_m = \left[3\left(\frac{V_L{}^3 V_S{}^3}{V_S{}^3 + 2V_L{}^3}\right)\right]^{1/3} \quad (13)$$

$$Y = \rho(V_L)^2 \quad (14)$$

$$G = \rho(V_S)^2 \quad (15)$$

$$\sigma = \frac{(Y-2G)}{2(Y-G)} \quad (16)$$

$$C_{12} = \frac{\sigma C_{11}}{1-\sigma} \quad (17)$$

$$B = (C_{11} + 2C_{12})/3 \quad (18)$$

$$\theta_D = \frac{hV_m}{K_B}\left[\frac{3\rho q N_A}{4\pi M}\right]^{1/3} \quad (19)$$

where, h = Planks constant, M = Molecular weight, K_B = Boltzmann constant, ρ = density, and q = Number of atoms in one formula unit.

Table 3 Elastic parameters of sintered $CoFe_2O_4$ spinel ferrites

Parameters	Sintering Temperture		
	400 °C	700 °C	900 °C
$C_{11} \times 10^{11}$ (GPa)	2.11	2.05	2.01
V_L (m/s)	6299.12	6229.85	6177.24
V_S (m/s)	3636.80	3596.81	3566.43
V_m (m/s)	4037.54	3993.14	3959.41
$Y \times 10^{11}$ (GPa)	2.11	2.05	2.01
$G \times 10^{11}$ (GPa)	0.7017	0.6820	0.6694
σ	0.25	0.25	0.25
$C_{12} \times 10^{11}$ (GPa)	0.7017	0.6820	0.6694
$B \times 10^{11}$ (GPa)	1.17	1.14	1.12
θ_D (K)	549.46	542.26	537.39

Estimated values of elastic stiffness constants (C_{11} & C_{12}) for different sintering temperature are listed in Table 3. It has been observed a decrease trend in stiffness constants with an increase in sintering temperature. The stiffness constants mainly depend on force constants and strength of atomic bonding. The decrement in C_{11} & C_{12} may be attributed due to increase in lattice volume and weakening of atomic bonding between Co^{2+}, Fe^{3+}, and O^{2-} ions [34]. Elastic moduli (Y, G, B) are found to decrease with increase in sintering temperature. The decrease in elastic moduli may be due to decrease in atomic binding force [31,34]. The longitudinal wave velocity, transverse wave velocity, and mean velocity estimated from equations 11, 12, and 13 respectively and listed in Table 3. It is observed that elastic wave velocities decreased with increase in sintering temperature. This is accounted weakening of bonds between Co^{2+}, Fe^{3+}, and O^{2-} ions or decrease in force constants with increase in sintering temperature [35]. The Poisson's ratio is observed to be constant for all sintering temperatures and it is found to be between -1.0 to 0.5 for isotropic elastic materials [35]. The Debye temperature (θ_D) found to be decreased with increase in sintering temperature. The decrease in θ_D with increase in sintering temperature may be due to absorption heat partly of the conduction electron [31].

4. Conclusion

Cobalt ferrite nanoparticles were synthesized by using sol–gel auto combustion method and sintered at the different temperatures viz. 400 °C, 700 °C, and 900 °C. In the present work, structural and elastic properties are investigated with respect to sintering temperature. The XRD pattern confirms the cubic spinel structure without any impurity for all sintering temperatures. Cubic spinel phase was obtained at a very low sintering temperature (400 °C). The crystallite size increases from 15.99 nm to 69.08 nm and grain size increases with increase in sintering temperature from 56.28 nm to 107.54 nm indicating that grains are formed due to agglomeration of several crystallites. The lattice parameters and lattice volume increases while X-ray density decreases with increasing sintering temperature. The FTIR spectrum confirmed the formation of spinel ferrite structure. Elastic moduli (Y, G, B), elastic wave velocities (V_l, V_t, V_m), and Debye temperature (θ_D) are found to be decreased with increase in sintering temperature.

References

[1] S.J. Salih, W.M. Mahmood, Review on magnetic spinel ferrite (MFe_2O_4) nanoparticles: From synthesis to application, Heliyon 9(6) (2023) e16601.

[2] J. Massoudi, M. Smari, K. Nouri, E. Dhahri, K. Khirouni, S. Bertaina, L. Bessais, E.K. Hlil, Magnetic and spectroscopic properties of Ni–Zn–Al ferrite spinel: from the nanoscale to microscale, RSC Adv. 10(57) (2020) 34556–34580.

[3] S. Dlamini, A. Nhlapo, T. Moyo, Remarkable structural and magnetic properties of nickel-zinc spinel ferrites synthesized by refluxing method, Next Mater. 8 (2025) 100602.

[4] R. Ranga, A. Kumar, P. Kumari, P. Singh, V. Madaan, K. Kumar, Ferrite application as an electrochemical sensor: A review, Mater. Charact. 178 (2021) 111269.

[5] T. Tatarchuk, A. Shyichuk, N. Danyliuk, M. Naushad, V. Kotsyubynsky, V. Boychuk, Cobalt ferrite as an electromagnetically boosted metal oxide hetero-Fenton catalyst for water treatment, Chemosphere 326 (2023) 138364.

[6] A.R. Liandi, A.H. Cahyana, A.J.F. Kusumah, A. Lupitasari, D.N. Alfariza, R. Nuraini, R.W. Sari, F.C. Kusumasari, Recent trends of spinel ferrites (MFe_2O_4: Mn, Co, Ni, Cu, Zn) applications as an environmentally friendly catalyst in multicomponent reactions: A review, CSCEE 7 (2023) 100303.

[7] K. Poon, G. Singh, Enhancing crystallinity and magnetic properties of cobalt ferrite nanoparticles via thermal oxidation, Chem. Nano. Mat. 10 (2024) e202400168.

[8] M.N. Kiani, M.S. Butt, I.H. Gul, M. Saleem, M. Irfan, A.H. Baluch, M.A. Akram, M.A. Raza, Synthesis and characterization of Cobalt-Doped ferrites for biomedical applications, ACS Omega 8(4) (2023) 3755–3761.

[9] V. Bhagwat, A.V. Humbe, S. More, K. Jadhav, Sol-gel auto combustion synthesis and characterizations of cobalt ferrite nanoparticles: Different fuels approach, Mater. Sci. Eng. B 248 (2019) 114388.

[10] I. Jhala, J.D. Baraliya, S.R. Ajudiya, P. Bardapurkar, N. Barde, N. Shah, P. Solanki, A.R. Tanna, H. Joshi, Structural and magnetic properties of cobalt ferrite nanoparticles synthesized by auto–combustion sol–gel method, Next Mater. 9 (2025) 101120.

[11] K.I. Nassar, S.S. Teixeira, M.P.F. Graça, Sol–Gel-synthesized metal oxide nanostructures: advancements and prospects for spintronic applications—a comprehensive review, Gels 11(8) (2025) 657.

[12] S.M. Hashemi, Z. Ataollahi, S. Hasani, A. Seifoddini, Synthesis of the cobalt ferrite magnetic nanoparticles by sol–gel auto-combustion method in the presence of egg white (albumin), J. Sol-Gel Sci. Technol. 106(1) (2023) 23–36.

[13] S. Sharma, R.K. Sharma, N. Negi, Sintering temperature effect on cation distribution and functional properties of metallo-organic decomposition processed $NiCo_{0.02}Cu_{0.02}Mn_{0.1}Fe_{1.8}O_4$ ferrites, Ceram. Int. 51(28) (2025) 57196-57215.

[14] P. More, S. Kadam, P. Lokhande, G. Jangam, S. Patange, D. Satpute, Effect of sintering temperature on the structural, morphological, and the magnetic properties of $Ni_{0.25}Cu_{0.55}Zn_{0.20}Fe_2O_4$ nano ferrite, J. Magn. Magn. Mater. 586 (2023) 171192.

[15] S. Xavier, M.K. Jiji, S. Thankachan, E.M. Mohammed, Effect of sintering temperature on the structural and electrical properties of cobalt ferrite nanoparticles, AIP Conf. Proc. 1576 (2014) 98–101.

[16] Y. Han, A. Sun, X. Pan, W. Zhang, X. Zhao, Effect of different sintering temperatures on structural and magnetic properties of ZN–Co ferrite nanoparticles, J. Supercond. Nov. Magn., 32(12) (2019) 3823–3830.

[17] B.D. Stojanovic, A.S. Dzunuzovic, N.I. Ilic, Review of methods for the preparation of magnetic metal oxides, In: Magnetic, Ferroelectric, and Multiferroic Metal Oxides, Elsevier, USA, 2018, pp.333–359.

[18] D. Pal, Synthesis of cobalt ferrite nanoparticles and their applications in hyperthermia therapy, J. Adv. Sci. Res. 14(02) (2023) 86–91.

[19] D. Narsimulu, O. Padmaraj, E.S. Srinadhu, N. Satyanarayana, Synthesis, characterization and electrical properties of mesoporous nanocrystalline $CoFe_2O_4$ as a negative electrode material for lithium battery applications, J. Mater. Sci.: Mater. Electron. 28(22) (2017) 17208–17214.

[20] A. Zubair, Z. Ahmad, A. Mahmood, W. Cheong, I. Ali, M.A. Khan, A.H. Chughtai, M.N. Ashiq, Structural, morphological and magnetic properties of Eu-doped $CoFe_2O_4$ nano-ferrites, Result Phys. 7 (2017) 3203–3208.

[21] M. Ajmal, M. Islam, G.A. Ashraf, M.A. Nazir, M. Ghouri, The influence of Ga doping on structural magnetic and dielectric properties of $NiCr_{0.2}Fe_{1.8}O_4$ spinel ferrite, Physica B Condens. Matter 526 (2017) 149–154.

[22] K. Praveena, K. Sadhana, S. Matteppanavar, Hsiang-Lin Liu, Effect of sintering temperature on the structural, dielectric and magnetic properties of $Ni_{0.4}Zn_{0.2}MN_{0.4}Fe_2O_4$ potential for radar absorbing, J. Magn. Magn. Mater. 423 (2017) 343–352.

[23] C. Mondal, A. Dutta, A. Sinha, Structural interpretation of sintering temperature effect on optical and electrical properties of Pr^{3+}-Substituted nickel ferrites, Phys. Status Solidi A 220(17) (2023) 2300263.

[24] S. Akter, M.N.I. Khan, F. Ferdous, H.N., Das, M.K. Alam, M.A.Rahman, T. Hasan, I.M. Syed, Unveiling the role of sintering temperatures in the physical properties of CU-MG ferrite nanoparticles for photocatalytic application, Heliyon, 10(23) (2024) e40771.

[25] C.E. Ribeiro, M. Vinícius-Araújo, A.F. Bakuzis, Multicore manganese ferrite nanoparticles for Theranostics, ACS Appl. Nano Mater. 8 (2025) 7061–7072.

[26] Q. Lin, J. Lin, Y. He, R. Wang, J. Dong, The structural and magnetic properties of gadolinium doped $CoFe_2O_4$ nanoferrites, J. Nanomater. 2015 (2015) 1-6.

[27] V. Rathod, A. Anupama, R.V. Kumar, V. Jali, B. Sahoo, Correlated vibrations of the tetrahedral and octahedral complexes and splitting of the absorption bands in FTIR spectra of Li-Zn ferrites, Vib. Spectrosc. 92 (2017) 267–272.

[28] E. Wolska, P. Piszora, W. Nowicki, J. Darul, Vibrational spectra of lithium ferrites: infrared spectroscopic studies of Mn-substituted $LiFe_5O_8$, Int. J. Inorg. Mater. 3(6) (2001) 503–507.

https://doi.org/10.30799/jnst.365.26110101

Cite this Article as: Ravindra N. Chikhale, Vikas S. Shinde, Rietveld structure refinement and effect of sintering temperature on elastic properties of cobalt nano ferrite, J. Nanosci. Tech. 11(1) (2026) 1022-1026.

[29] T.S. Almutairi, Unraveling the complex interplay of phase transitions in spinel ferrites: A comprehensive quantum mechanical vibrational study of $ZnFe_2O_4$, ACS Omega 8(40) (2023) 36999–37010.
[30] E.H. El-Ghazzawy, Effect of heat treatment on structural, magnetic, elastic and optical properties of the co-precipitated $Co_{0.4}Sr_{0.6}Fe_2O_4$, J. Magn. Magn. Mater. 497 (2020) 166017.
[31] S. Nasrin, S.M. Khan, M.A. Matin, M.N.I. Khan, A.K.M. Akther Hossain, M.D. Rahaman, Synthesis and deciphering the effects of sintering temperature on structural, elastic, dielectric, electric and magnetic properties of magnetic $Ni_{0.25}Cu_{0.13}Zn_{0.62}Fe_2O_4$ ceramics, J. Mater. Sci.: Mater. Electron. 30(11) (2019) 10722–10741.
[32] M.A. Amer, T. Meaz, S. Attalah, F. Fakhry, Influence of heat treatment on magnetic, structural and elastic properties of as-prepared Mg-nanoferrites, J. Magn. Magn. Mater. 401 (2016) 150-158.
[33] H. Khedri, A. Gholizadeh, Experimental comparison of structural, magnetic and elastic properties of $M_{0.3}Cu_{0.2}Zn_{0.5}Fe_2O_4$ (M = Cu, Mn, Fe, Co, Ni, Mg) nanoparticles, Appl. Phys. A 125(10) (2019) 709.
[34] M.A. Amer, T.M. Meaz, S.S. Attalah, A.I. Ghoneim, Structural phase transition of as-synthesized Sr–Mn nano ferrites by annealing temperature, J. Magn. Magn. Mater. 393 (2015) 467–478.
[35] A.V. Anupama, V. Rathod, V.M. Jali, B. Sahoo, Composition dependent elastic and thermal properties of Li Zn ferrites, J. Alloys Compd. 728 (2017) 1091–1100.

https://doi.org/10.30799/jnst.365.26110101

Cite this Article as: Ravindra N. Chikhale, Vikas S. Shinde, Rietveld structure refinement and effect of sintering temperature on elastic properties of cobalt nano ferrite, J. Nanosci. Tech. 11(1) (2026) 1022-1026.